Title

Histopathologic and Transcriptomic Profiling Identifies Novel Trophoblast Defects in Patients With Preeclampsia and Maternal Vascular Malperfusion.

Journal

Modern pathology : an official journal of the United States and Canadian Academy of Pathology, Inc, 36(2)

ISSN

0893-3952

Authors

Horii, Mariko
To, Cuong
Morey, Robert
et al.

Publication Date

2023-02-01

DOI

10.1016/j.modpat.2022.100035

Peer reviewed

HHS Public Access

Author manuscript

Mod Pathol. Author manuscript; available in PMC 2023 April 07.

Published in final edited form as:

Mod Pathol. 2023 February ; 36(2): 100035. doi:10.1016/j.modpat.2022.100035.

Histopathologic and Transcriptomic Profiling Identifies Novel Trophoblast Defects in Patients With Preeclampsia and Maternal Vascular Malperfusion

Mariko Horii[a,b], **Cuong To**[b,c], **Robert Morey**[b,c], **Marni B. Jacobs**[b,c], **Yingchun Li**[a,b], **Katharine K. Nelson**[a,b], **Morgan Meads**[a,b], **Brent A. Siegel**[a], **Donald Pizzo**[a], **Rebecca Adami**[c], **Kathy Zhang-Rutledge**[c], **Leah Lamale-Smith**[c], **Louise C. Laurent**[b,c], **Mana M. Parast**[a,b,*]

[a]Department of Pathology, University of California San Diego, La Jolla, California

[b]Sanford Consortium for Regenerative Medicine, University of California San Diego, La Jolla, California

[c]Department of Obstetrics, Gynecology, and Reproductive Sciences, University of California San Diego, La Jolla, California

Abstract

Preeclampsia (PE) is a heterogeneous disease for which the current clinical classification system is based on the presence or absence of specific clinical features. PE-associated placentas also show heterogeneous findings on pathologic examination, suggesting that further subclassification is possible. We combined clinical, pathologic, immunohistochemical, and transcriptomic profiling of placentas to develop integrated signatures for multiple subclasses of PE. In total, 303 PE and 1388 nonhypertensive control placentas were included. We found that maternal vascular malperfusion (MVM) in the placenta was associated with preterm PE with severe features and with small-for-gestational-age neonates. Interestingly, PE placentas with either MVM or no histologic pattern of injury showed a linear decrease in proliferative ($p63^+$) cytotrophoblast per villous area with increasing gestational age, similar to placentas obtained from the nonhypertensive patient cohort; however, PE placentas with fetal vascular malperfusion or villitis of unknown etiology lost this phenotype. This is mainly because of cases of fetal vascular malperfusion in placentas

*Corresponding author: mparast@health.ucsd.edu (M.M. Parast).

Author Contributions

M.H. and M.M.P. designed the research. K.K.N. and M.M. recruited patients and collected clinical information. M.B.J. collected and managed the database. R.A., K.Z.-R., L.L.-S., and L.C.L were involved in the review of data within the obstetrics registry and adjudication of hypertensive disease of pregnancy. M.M.P. reviewed all placental pathology data and performed all coding of data into the obstetrics registry. M.H., M.B.J., and M.M.P. performed statistical analysis of clinical and pathologic data. B.S. and D.P. performed all immunohistochemical staining. M.H., Y.C.L., and D.P. performed immunohistochemical data analysis. M.H., C.T., R.M., and L.C.L. performed all computational data analyses. M.H., M.B.J., C.T., R.M., and M.M.P. wrote the manuscript text. All authors reviewed the final version of the manuscript.

Declaration of Competing Interest

The authors declare no conflicts of interest.

Ethics Approval and Consent to Participate

Clinical data and placental samples were collected under the protocol for the Perinatal Biorepository, approved by the Human Research Protections Program Committee of the University of California San Diego Institutional Review Board (IRB number: 181917X).

Supplementary Material

The online version contains supplementary material available at https://doi.org/10.1016/j.modpat.2022.100035.

of patients with preterm PE and villitis of unknown etiology in placentas of patients with term PE, which are associated with a decrease or increase, respectively, in the cytotrophoblast per villous area. Finally, a transcriptomic analysis identified pathways associated with hypoxia, inflammation, and reduced cell proliferation in PE-MVM placentas and further subclassified this group into extravillous trophoblast-high and extravillous trophoblast-low PE, confirmed using an immunohistochemical analysis of trophoblast lineage-specific markers. Our findings suggest that within specific histopathologic patterns of placental injury, PE can be subclassified based on specific cellular and molecular defects, allowing the identification of pathways that may be targeted for diagnostic and therapeutic purposes.

Keywords

preeclampsia; maternal vascular malperfusion; fetal vascular malperfusion; cytotrophoblast; syncytiotrophoblast; extravillous trophoblast

Introduction

Preeclampsia (PE) is a multifactorial, multisystem, and progressive pregnancy disorder, which is characterized by new-onset hypertension with end-organ dysfunction, appearing after 20 weeks of gestation.[1] This disease is associated with not only increased risks of perinatal morbidity and mortality but also development of metabolic and cardiovascular diseases later in life in both mothers and babies.[2,3]

The underlying pathophysiology of PE involves both maternal and placental/fetal factors; the placental contribution is supported by the observations that pregnancies complicated by complete hydatidiform moles (in which there is placental but not fetal tissue) are frequently affected by PE[4] and that PE resolves after delivery of the placenta.[1,5,6] The “2-stage theory” of PE pathogenesis states that the disease is a result of initial ischemia-reperfusion injury caused by poor placentation (for which maternal endothelial dysfunction is a risk factor), followed by secretion of factors by the affected placenta that stimulate vascular inflammation, leading to maternal systemic disease.[5] Poor placentation in the first stage involves abnormal development of epithelial cells of the placenta, called trophoblast, which comprise 3 main subpopulations: cytotrophoblast (CTB), syncytiotrophoblast (STB), and extravillous trophoblast (EVT).[5,7] The CTB comprises bipotential trophoblast progenitor cells that can give rise to either multinucleated and hormone-secreting STB, which is involved in gas and nutrient exchange at the maternal-fetal interface, or invasive EVT, which anchors the placenta to the uterine wall and remodels spiral arterioles in the maternal decidua to establish maternal blood supply to the fetoplacental unit.[7,8] Abnormal development and/or function of the latter cell type, EVT, leads to shallow implantation within the uterus and is most strongly associated with early-onset PE, which is often accompanied by fetal growth restriction.[9]

Clinically, PE is categorized based on the presence or absence of specific clinical features (ie, with or without severe features, respectively) and as primary versus superimposed (without or with preexisting chronic hypertension, respectively).[1,5,6,10] The gestational age (GA) at disease onset (early-onset [EO] or late-onset [LO] PE, often defined based on a

cutoff of 34 weeks of GA) is also considered in decisions about the clinical management of PE. The assessment of predisposing risk factors (including race, nulliparity, family history, use of assisted reproductive technologies, and preexisting medical conditions) suggests that PE is substantially more heterogeneous than the small number of criteria used for clinical management would imply, pointing toward molecular, immunologic, genetic, and environmental contributions to this syndrome.[5,6,11–15] Because of this heterogeneity, the few currently available diagnostic biomarkers for this disease, such as the ratio of soluble fms-like tyrosine kinase 1 (sFlt-1) to placental growth factor (PlGF), have low positive predictive values within the general pregnant population[16] and are, therefore, useful for exclusion but not for prediction of the disease.[17,18]

Recently, Redline et al[19] grouped placental pathologic findings, as defined by the Amsterdam Placental Workshop Group Consensus Statement (APWGCS),[20] into 4 main categories of placental injury—maternal vascular malperfusion (MVM), fetal vascular malperfusion (FVM), acute chorioamnionitis (ACA), and villitis of unknown etiology (VUE)—in order to standardize placental pathologic diagnosis and incorporate this into the classification of obstetric diseases.[19,20] MVM is a pattern of injury that is thought to arise from abnormal remodeling of maternal spiral arterioles by EVT, leading to abnormal maternal blood flow and ischemic damage to the chorionic villi.[19,21] MVM placentas are usually small (with a placental disc weight of <10th percentile for GA) and can show accelerated villous maturation (AVM) and/or villous infarction. These lesions develop secondary to or in association with hypertensive changes in maternal vessels, called decidual arteriopathy, a lesion that ranges from persistence of vascular smooth muscle to chronic perivascular inflammation, fibrinoid necrosis of the vascular wall, acute atherosis, and thrombosis.[22] FVM is characterized by obstruction and/or thrombosis of large fetal blood vessels, which can lead to avascular and hyalinized chorionic villi.[19,23] ACA is characterized by a maternal acute inflammatory response triggered by ascending infection within the fetal membranes and amniotic fluid.[19,24] VUE is characterized by maternal T-cell infiltration and/or increased numbers of fetal Hofbauer cells (macrophages) in response to fetal antigens in the villous stroma, which lead to breach of the vasculosyncytial membrane, damaging the gas-nutrient exchange interface.[19,25] Of these 4 categories, MVM is most often associated with maternal hypertensive disorders of pregnancy, including PE.[19,26–28] However, not all patients with PE have placentas with evidence of MVM, and not all MVM placentas are from patients with PE.[19,26] In addition, the prevalence of MVM is known to be higher in cases of EO-PE with severe features, further highlighting the underlying differences in biological processes leading to EO- versus LO-PE.[10,26,29,30] Studies connecting PE to other relevant patterns of placental injury, particularly FVM and VUE, are still emerging.

Finally, Leavey et al[31,32] previously applied unsupervised analytical methods to microarray-based RNA profiling data from placental tissues to divide PE into 3 distinct molecular subgroups. These include “canonical” PE, characterized by changes in the expression of genes associated with angiogenesis and placental ischemia; “immunologic” PE, characterized by changes in the expression of genes associated with immune response and allograft rejection; and “maternal” PE, wherein placental tissue shows no significant enrichment of any gene ontologies. A retrospective evaluation of placental pathology in each of these 3 categories revealed specific patterns of placental injury.[33,34] Canonical PE was

characterized by AVM and infarction, immunologic PE was characterized by villitis and increased perivillous fibrin deposition, and maternal PE showed no specific histopathologic changes.[33,34] These studies have clearly demonstrated the utility of molecular profiling in the identification of subclasses of PE, which may have a basis in the underlying pathophysiologic heterogeneity of this disease. Nevertheless, these studies have been limited by their use of microarray-based RNA profiling data, aggregated from multiple centers, and having only retrospectively been connected to placental pathologic findings.

In this study, we set out to apply a supervised classification method, focused on identifying subclasses of primary (non-superimposed) PE with severe features based on histopathologic, cellular, and, finally, molecular phenotyping. We began with a cohort of patients, with and without a diagnosis of primary PE with severe features from a single center, with prospectively collected clinical and placental pathologic assessments, following established criteria uniformly applied to all cases. We continued with histopathologic subclassification of these cases based on the APWGCS patterns of placental injury, followed by an immunohistochemical assessment of cellular phenotypes and a subsequent molecular level analysis using RNA sequencing (RNA-seq)-based transcriptomic profiling. Our findings address discrepancies in the literature, particularly with regard to morphologic and cellular phenotypes of PE-associated placentas, while also providing novel insights into PE heterogeneity at both cellular and molecular levels. The latter have the potential to contribute to improvements in the identification of diagnostic biomarkers and therapeutic targets, which are based on underlying disease pathophysiology.

Materials and Methods

Case Selection

All patients included in the study delivered at hospitals affiliated with University of California San Diego (UCSD) between January 2010 and November 2020 and gave informed consent for collection of clinical data (including placental pathology) and placental tissue at delivery. A total of 3054 patients consented during this period, of whom 2654 had complete demographic, clinical (including adjudicated diagnosis regarding hypertensive disorder of pregnancy), and placental pathology data available in an associated RedCap-based obstetric registry (Fig. 1). The clinical diagnosis of hypertensive disease was adjudicated by 2 practicing obstetricians, at least 1 of whom is a board-certified maternal-fetal medicine specialist (R.A., K.Z.R., L.L.S., L.C.L.). Out of the 2654 patients, an additional 543 were excluded because of the onset of hypertension or proteinuria before 20 weeks of gestation. Of the remaining patients, 303 met the criteria for primary PE with severe features based on the definition by American College of Obstetricians and Gynecologists,[1] with 420 excluded because of absence of criteria for severe disease. The remaining 1388 served as the nonhypertensive reference (control) group. Placental examinations, including gross and histologic examinations, were performed through either the hospital (for placentas with a clinical indication for an examination) or the research core (for placentas without such indications). Regardless of gross examination and processing, all the placentas underwent a histologic examination performed by a single perinatal pathologist (M.M.P.).

Obstetric Data

The specific demographic data collected included maternal age at delivery, race and ethnicity, gravidity, GA at delivery, fetal sex, birth weight, and mode of delivery. PE with severe features was characterized by new onset of hypertension (≥140/90 mm Hg) with at least 1 of the following features: hypertension ≥ 160/110 mm Hg, proteinuria ≥ 5 g, impaired liver function (twice the transaminase upper limit), low platelet count ($\leq 1.0 \times 10^5$ cells/μL), or renal insufficiency (Cr ≥ 1.2 mg/dL), diagnosed after 20 weeks of gestation. The reference groups were defined based on the absence of hypertension and any other features of PE with severe features. The birth weight percentile was calculated based on the Hadlock formulation adjusted for GA.[35,36] Small for gestational age (SGA) was categorized as a birth weight of <10th percentile for GA.

Histopathologic Examination

The placental examination and sampling were performed based on the Amsterdam Consensus Statement.[20] The trimmed weight of the unfixed placental disc (without an attached cord and membranes) was measured and categorized as small (≤10th percentile for GA), normal (11th-89th percentile for GA), or large (≥90th percentile for GA).[37] Only minimal obstetric information was available at the time of histologic evaluation, including GA, mode of delivery, and indication for placental examination (ie, diabetes, PE, and fetal growth restriction).

Pathologic Criteria

“All-MVM” was defined as any small placenta with at least 1 of the following 4 findings: AVM, infarction, decidual arteriopathy, and retroplacental/marginal hematoma. “Pure” MVM was defined as MVM without concurrent evidence of FVM or VUE. MVM + FVM was defined as MVM with concurrent evidence of FVM but without evidence of VUE. MVM + VUE was defined as MVM with concurrent evidence of VUE but without evidence of FVM. FVM was defined as any case with fetal vascular thrombosis or avascular or near-avascular villi (AV) of any grade but without evidence of VUE and not meeting the criteria for MVM (ie, “pure” FVM). VUE was defined as any case with chronic villitis of any grade that did not meet the criteria for MVM. Normal pathology was defined as any case that did not meet the criteria for MVM, FVM, or VUE (Supplementary Table S1).

Immunohistochemistry

All immunohistochemical stains were performed at UCSD Advanced Tissue Technology Center. p63 staining was performed on 91 PE placentas and 99 nonhypertensive control placentas; the latter were selected to match the GA range of the PE placentas and because of lack of any placental disc lesions (which could otherwise affect the CTB number per villous area). CD68 staining was performed on 5 placentas with VUE. Validation of the RNA-seq data was performed on a total of 15 PE placentas (6 EVT^{hi}/STB^{lo} placentas and 9 EVT^{lo}/STB^{hi} placentas) and 8 normal, term placentas. One block with representative noninfarcted placental disc tissue from each case was selected. Formalin-fixed, paraffin-embedded placental tissue sections of 5 μm were stained with mouse anti-p40 (ΔNp63-specific antibody, clone BC28; 1:300; ACI3066C, Biocare Medical), mouse anti-CD68

(clone KP1; 1:1800; M0814, Agilent Dako), mouse anti-HLA-G (clone 4H84; 1:6000; ab52455, Abcam), or rabbit antiplacental lactogen (1:6000; ab15554, Abcam) antibodies using a Ventana Discovery Ultra automated immunostainer (Roche Diagnostics) with standard antigen retrieval and reagents per the manufacturer's protocol.

For quantification of proliferative CTB per villous area, the immunostained slides were scanned using a Zeiss slide scanner. Tissue studio (Definiens) was used to calculate the number of $p63^+$ nuclei per villous trophoblast area (μm^2) following the software instructions. In brief, 1 randomly selected slide was used for training the software, with annotation of specific regions of interest (ie, maternal blood space, trophoblast layer, villous stroma, as well as chorionic and basal plates). Then, a cell-based analysis was performed using automated counting of $p63^+$ and $p63^-$ nuclei as well as measurement of the area of trophoblast layer based on morphology. The CTB number was calculated as the number of $p63^+$ nuclei per trophoblast area (μm^2).

For quantification of CTB per villous area, in regions with and without AV, a total of 6 cases of PE with FVM were selected (placentas delivered between 26 and 38 weeks, 4 with MVM + FVM and 2 with pure FVM). The AV-affected area was marked based on morphology by a perinatal pathologist (M.M.P.). The number of $p63^+$ nuclei per villous area was calculated, and the paired *t* test was used to compare the count in AV- and non-AV—affected areas within the same placenta. For the quantification of CTB per villous area, in regions with and without chronic inflammation (CI), a total of 5 cases of PE with VUE were used (placentas delivered between 36 and 40 weeks, all with pure VUE). The CI-affected area was marked based on morphology by a perinatal pathologist (M.M.P.) and confirmed based on increased levels of CD68 (a marker for macrophages) staining. The number of $p63^+$ nuclei per villous area was calculated, and the paired *t* test was used to compare the count in CI− and non-CI —affected areas within the same placenta.

RNA Isolation From Placental Tissue and RNA-Seq

Total RNA was isolated from placental villous tissue (avoiding the chorionic and basal plates) using the mirVana RNA Isolation Kit (ThermoFisher). The RNA concentration was measured using the Qubit RNA BR assay kit (ThermoFisher). The RNA integrity was checked using the RNA 6000 Nano chip read by a 2100 bioanalyzer (Agilent). All samples had an RNA integrity number of >7.0. RNA-seq libraries were prepared using the TruSeq Stranded Total RNA Sample preparation kit with Ribo-Zero Gold (Illumina) at IGM Genomics Center, UCSD. The libraries were pooled and sequenced on NovaSeq 6000 (Illumina) with PE100 to an average depth of 25,000,000 uniquely mapped reads. Quality control was performed using FastQC (version 0.11.3). The reads were mapped to GRCh38.89 (Ensembl) using STAR (version 2.5.3a)[38] on Extreme Science and Engineering Discovery Environment.[39] The STAR parameters used were as follows: –runThreadN 24 –sjdbOverhang 99 –genomeDir ref_ensembl_GRCh38_89/star_index –sjdbGTFtagExonParentGene gene_id –sjdbGTFfile ref_ensembl_GRCh38_89/Homo_sapiens.GRCh38.89.gtf –outSAMtype BAM Unsorted SortedByCoordinate –outReadsUnmapped Fastx –quantMode Gene-Counts. Ensembl genes with at least 10 counts in 25% of the samples were filtered for the analysis. Normalization

and the differential expression analysis (DEA) were performed using the R (version 4.0.3) package DESeq2 (version 1.30.1).[40] BiomaRt (version 2.42.1) was used to convert Ensembl gene identification numbers to Human Genome Organization gene names[41]; the gene set enrichment analysis was performed using the R (version 4.0.3) package Fast Gene Set Enrichment Analysis (version 1.16.0), and a gene ontology analysis was performed using Enrichr.[42]

Single-Cell RNA-seq for Deconvolution of Bulk RNA-seq

Previously reported, aligned, filtered, and quantified single-cell RNA-seq data obtained from 4 normal-term placentas (tissue from a total of 6 placental parenchymal biopsies, with 2 samples collected from 2 areas of placental disc) and 4 EO-PE placentas were downloaded from the European Genome-Phenome Archive (accession no. EGAS00001002449).[43] These data were used to create a cell type deconvolution signature matrix for CIBERSORT (cell-type identification by estimating relative subsets of RNA transcripts) to estimate the abundance of member cell types in our bulk RNA-seq data.[44] After combining the single-cell data sets, the data were further filtered to contain only genes detected in at least 10 cells and cells that express at least 250 different genes. The data were then normalized by library size, batch corrected using regression on counts, and filtered for highly variable genes, resulting in a total of 34,786 cells and 2232 genes. The principal component analysis was used to determine the number of principal components to use in the nearest neighbor analysis. The data were then clustered using the Louvain algorithm and visualized using t-distributed stochastic neighbor embedding, resulting in 18 clusters. To determine cluster cell identity, the marker genes for each cluster were ranked by comparing each cluster with all other clusters using the *t* test with variance overestimation. The average gene expression for each gene in each cluster was then used as the input file (signature matrix) for CIBERSORT.[44] All single-cell analyses were performed using Scanpy (version 1.4.3).[45] The CIBERSORT output is provided in Supplementary Table S2. “All trophoblast” (“all troph” for short) was calculated based on the sum of CTB, STB, and EVT, with the proportion of EVT or STB calculated based on EVT/all troph or STB/all troph. A scatter plot was made using GA and the calculated values (EVT/all troph or STB/all troph) of the PE placental samples. The 2 groups, EVT^{hi}/STB^{lo} and EVT^{lo}/STB^{hi}, were selected based on a hierarchical clustering analysis of the calculated values using both EVT/all troph and STB/all troph, first determining EVT^{hi}/STB^{lo} cases and then identifying GA-matched cases for a second hierarchical clustering analysis to validate the EVT^{lo}/STB^{hi} cases. DEA was performed on these 2 groups (Supplementary Table S3), and major histocompatibility complex, class I, G (HLA-G) and chorionic omatomammotropin hormone 1 (CSH1, human placental lactogen) were selected for validation of the EVT^{hi}/STB^{lo} and EVT^{lo}/STB^{hi} groups, respectively.

Statistical Analysis

Statistical analyses were performed using the SPSS software (version 27.0; IBM). Testing of normality was performed using the Shapiro-Wilk test. The Mann-Whitney *U* or Kruskal-Wallis test was applied to all nonparametric data and student *t* test to all parametric data with continuous variables. The Pearson χ^2 test was used for categorical variables, and when >20% of the expected counts were <5, the Fisher exact test was used. All

statistical tests were 2 sided, with *P* values <.05 considered statistically significant. Linear regression models were used, after ensuring that the data were normally distributed, to analyze the relationship between the value of positive CTB number per villous area and GA; furthermore, the R^2, unstandardized β coefficient, and *P* value were estimated. The box plots showed the median with the center line; mean as the cross mark, with the box indicating the upper and lower quartiles; the whiskers indicating the maximum and minimum values; and the outlier or single data point marked as circles. DEA was performed using DESeq2, and an adjusted *P* value of <.05 was considered differentially expressed.

Results

Patient Cohort

The overall cohort included 3054 pregnant women who consented to chart review and biospecimen collection for our ongoing Perinatal Biorepository between January 2010 and November 2020 and for whom adjudicated hypertensive diagnoses and placental pathologic data were available (Fig. 1). After removal of cases with incomplete pregnancy information or multiple gestations, there remained 2654 patients with singleton pregnancies, of whom an additional 543 were excluded because of the onset of hypertension or proteinuria before 20 weeks of gestation. Of the remaining patients, 303 met the criteria for primary PE with severe features, defined based on the definition by American College of Obstetricians and Gynecologists,[1] with another 420 patients excluded because of the absence of proteinuria or other evidence of PE-associated end-organ damage (elevated creatinine levels, low platelet counts, or elevated liver function enzyme levels). The remaining 1388 cases served as the nonhypertensive reference (control) group (Fig. 1). The maternal and neonatal characteristics are summarized in Supplementary Table S4. The maternal age and fetal sex did not differ between the groups, whereas the GA, gravidity, parity, and birth weight were lower and the rates of SGA neonates and preterm delivery were higher in the PE group. Somewhat surprisingly, the mode of delivery did not differ between the groups, suggesting a potential selection bias at enrollment. Our cohort included 38.2% Hispanic or Latino women, with the non-Hispanic population comprising White women as the largest subgroup (39.1%), followed by Asian (10.4%) and Black (4.5%) women. The prevalence of PE was higher in the Black (1.7-fold) and Native Hawaiian or Pacific Islander (3.3-fold) groups compared with that in the reference group. Overall, our study population confirmed the known characteristics of patients with PE, including a higher prevalence in primigravid women, and higher rates of SGA neonates and preterm birth.

Maternal Vascular Malperfusion is Associated With Primary Preeclampsia

We set out to assess the relationship between the clinical diagnosis of primary PE and pathologic patterns of placental injury, focusing on patterns previously associated with PE. To do this, we first defined the criteria for MVM, FVM, and VUE, including “pure” and “combined” patterns, based on the APWGCS definitions and as further specified by Redline et al[19] and others[20,26,29,46,47] (Supplementary Table S1). Then, we evaluated the presence of these patterns of injury in placentas from the PE and nonhypertensive cohorts. Similar to other studies,[19,26–28] we found a significantly higher prevalence of MVM in the placentas of patients with PE compared with the nonhypertensive reference group (odds ratio, 4.4; 95%

CI, 3.3–5.9) (Table 1). Interestingly, the other 2 patterns of injury, FVM and VUE, were present at similar rates in the PE and the reference groups (Table 1); however, as expected, the percentage of PE placentas with normal pathology was significantly lower than that of PE placentas in the reference group (odds ratio, 0.5; 95% CI, 0.4–0.6) (Table 1).

Because MVM is known to be associated with SGA neonates,[19,26,28] we also investigated the proportion of cases with this pattern of injury in PE and nonhypertensive patients with and without SGA neonates. We found that in both the PE cases and controls, the prevalence of delivering SGA neonates was higher in the subcohort with MVM. The other 2 patterns of FVM and VUE, however, were not enriched in the group with SGA neonates (Supplementary Table S5). As anticipated, the subcohort of PE with SGA neonates also showed the lowest proportion of histologically normal placentas, lacking any of these patterns of placental injury (Supplementary Table S5). Finally, we investigated whether differences in certain types of placental injury could affect the timing of delivery. We found that patients with MVM delivered significantly earlier than those with FVM, VUE, or normal placental pathology in both the PE ($P < .01$, an average of 33 vs 36–37 weeks of GA) and nonhypertensive cohorts ($P < .01$, an average of 36 vs 38–39 weeks of GA), with patients with MVM in the PE cohort faring the worst (Fig. 2). In order to exclude the possibility of SGA as a confounding factor associated with early delivery, we compared patients with and without SGA neonates within each pattern of placental injury. There was no difference in the timing of delivery between patients with and those without SGA neonates, regardless of the diagnosis of hypertension (Supplementary Fig. S1), indicating that SGA was not a confounding factor driving early delivery.

Overall, these data show a high prevalence of MVM pathology in PE placenta, although this lesion can also be present in the absence of maternal hypertensive disease. In addition, patients with MVM pathology in their placenta tend to deliver earlier, and those with this lesion are in fact more likely to deliver preterm in the setting of primary PE with severe features. Finally, MVM appears to be enriched in both patients with PE and nonhypertensive patients delivering an SGA baby.

Maternal Vascular Malperfusion Can Be Further Classified Into Pathologic Subgroups

MVM can be accompanied by other pathologic findings; however, few studies have addressed how these additional findings may alter or be associated with different clinical outcomes.[19,28] Therefore, we next evaluated MVM with and without the other 2 patterns of placental injury, FVM and VUE (Supplementary Table S1). We first investigated the proportion of each of the 3 subcategories, pure MVM, MVM + FVM, and MVM + VUE, between the PE cohort with MVM and the nonhypertensive cohort with MVM. We found no difference in the proportion of pure MVM and MVM + VUE (Table 2) but noted a higher proportion of MVM + FVM in the PE group than that in the nonhypertensive group (Table 2) (odds ratio, 2.7; 95% CI, 1.4–5.1). Next, we evaluated the proportion of these MVM subcategories in patients with PE and nonhypertensive patients with and without SGA neonates. We noted that the combined MVM + FVM pattern was particularly enriched in the group of PE patients with SGA neonates (Supplementary Table S6). Finally, we also found that these 3 subcategories can be distinguished by GA at delivery, with

pure MVM and MVM + FVM in PE placentas showing significantly earlier delivery than those with corresponding pathologic categories within the nonhypertensive controls (Fig. 3). Interestingly, patients with MVM + VUE tended to deliver near term, with no significant difference between the patients with PE and nonhypertensive patients (Fig. 3). Taken together, these findings show that MVM + FVM is most common in the setting of PE with SGA neonates and is associated with the lowest GA at delivery.

Pathologic Subcategories of Preeclampsia Can Be Further Defined Based on Cytotrophoblast Cell Number

Next, we decided to go beyond morphologic assessment and evaluate the PE placentas at the cellular level. We focused on CTB, the trophoblast progenitor cell in the placenta, because previous studies have shown conflicting data regarding CTB number, ranging from reports of no changes[48] to those of increased number of CTB or CTB proliferation in the setting of PE.[49,50] We stained 91 placentas from the patients with PE, who delivered between 24 weeks of gestation and term, and 99 placentas from the nonhypertensive patients, who delivered within the same GA window and lacked any placental disc lesions (Supplementary Table S7 for demographics of this patient subcohort), with antibodies against p63, a marker of villous CTB[51] to evaluate the number of CTB per villous area (μm2) (CTB/area) using an unbiased, automated counting method (see the Immunohistochemistry section). As expected, the placentas from the nonhypertensive patients without disc lesions showed a decrease in CTB/area with increasing GA (Fig. 4A, blue line; $R^2 = 0.73$; $P < .01$; unstandardized β coefficient, -4.28×10^{-5}). Overall, compared with the placentas of the nonhypertensive patients, those of the patients with PE did not differ in CTB/area ($P = .207$); however, similar to the placentas from the nonhypertensive patients, the trend line for the placentas from the patients with PE showed a decrease in CTB/area with advancing GA, with lower CTB/area for patients who delivered earlier in gestation and higher CTB/area for patients who delivered later in gestation (Fig. 4A, orange line; $R^2 = 0.52$; $P < .01$; unstandardized b coefficient, $-2.66 \times 10^{-}5$).

Given this observation, we further evaluated the CTB/area in the PE-associated placentas, separating the subgroups of MVM, FVM, VUE, or no pattern of placental injury (normal), as defined in Supplementary Table S1. We found that in this group, the linear decrease in CTB/area with increasing GA was statistically significant only in placentas with MVM or no pattern of placental injury but not in those with FVM or VUE (Supplementary Table S8). We speculated that this could be due to the effect of these lesions on CTB/area; however, these lesions are, for the most part, focal. Thus, we further evaluated a subset of these samples in more detail by measuring the CTB/area in adjacent areas with or without AV in FVM samples and with or without CI in VUE samples. In the FVM samples (n = 6), the AV-affected area showed significantly reduced CTB/area compared with the non-AV—affected area (Fig. 4B; $P = .04$), whereas in the VUE samples (n = 5), there was a significantly higher CTB/area in the CI-affected area than that in the non-CI—affected area (Fig. 4C; $P = .01$). These data suggest that different patterns of placental injury can affect CTB number in different ways, leading to heterogeneous conclusions when the disease is only defined based on clinical parameters. In summary, we conclude that the cellular phenotype in the placenta should be assessed based on a combination of clinical and pathologic definitions.

Preeclampsia Subclassification Based on Placental Transcriptomic Profiles

Finally, we went beyond cellular analysis, assessing the PE placentas at the transcriptome level using RNA-seq. Because the PE placentas were mostly enriched with MVM as the primary mode of placental injury, we first compared the placental transcriptomes of patients with PE and MVM (n = 26) with those of nonhypertensive patients with MVM (n = 18). DEA for this subcohort (Supplementary Table S9) was performed, controlling for GA, fetal sex, and the presence of SGA, resulting in 210 differentially expressed genes (Supplementary Table S10). Among these differentially expressed genes, the PE placentas with MVM showed significantly higher expression levels of genes known to be highly expressed in PE placentas, such as *LEP, FLT1, PAPPA2,* and *ENG* (6.2-, 3.1-, 2.1-, and 1.9-fold changes, respectively, compared with those in the control placentas). Using the DEA data, we next performed the gene set enrichment analysis, focusing on differences between the PE placentas with MVM and the control samples with MVM, using MSigDB hallmark gene sets.[52] A total of 12 gene sets were significantly enriched (adjusted $P < .05$), with 8 gene sets enriched in the control samples with MVM and 4 gene sets enriched in the PE placental samples with MVM (Fig. 5A). Among these, we noted pathways associated with cell proliferation or cell division (E2F targets, G2M checkpoint, MYC targets, and mitotic spindle) enriched in the control samples with MVM, with pathways associated with inflammation (interferon-α and ɣ signaling) and hypoxia to be conversely significantly enriched in the PE placentas with MVM. A leading-edge gene analysis (Supplementary Table S11) revealed nucleotide binding oligomerization domain containing 1 (*NOD1*), a gene in the interferon ɣ signaling pathway, to be enriched 1.3-fold in the PE placentas with MVM compared with that in the control placentas with MVM. Interestingly, *NOD1* was recently reported as a contributor to inflammation at the maternal-fetal interface, with increased expression levels in PE placentas.[53] In addition, 3 leading-edge genes within the hypoxia gene set deserve further mention here, including transmembrane protein 45A (*TMEM45A*), syndecan 3 (SDC3), and prolyl 4-hydroxylase subunit alpha 1 (*P4HA1*), which were enriched 2.4-,1.7-, and 1.5-fold, respectively, in the PE samples with MVM compared with those in the control placental samples with MVM (Supplementary Table S10). *TMEM45A* is known as a key modulator of hypoxia-induced chemoresistance,[54] found to be downstream of *STOX1* in a cell culture model of PE, and has been identified as a PE-associated gene.[55–57] Of the other 2 leading-edge genes, *SDC3* is known to be upregulated in the hypoxic tumor microenvironment,[58] and *P4HA1* is known as an upstream regulator of hypoxia-inducible factor, a transcription factor complex involved in mediating the effects of low oxygen levels.[59–61]

Given the differences in cell populations noted in the PE placentas based on p63 immunostaining, we reasoned that at least some of the changes in global gene expression were likely to have been due to changes in the proportion of various cell types within the sampled placental discs. Therefore, we sought to further evaluate cellular heterogeneity, focusing on assessing the proportion of different trophoblast cell types within the PE placentas with MVM (n = 26) (Supplementary Table S9). We performed a deconvolution analysis on our bulk placental RNA-seq data using publicly available placental single-cell RNA-seq data obtained by Tsang et al[43] using CIBERSORT.[44] While assessing the ratio of EVT to all troph signal, we found 2 distinct populations appearing in the PE samples with

MVM. Therefore, we applied the hierarchical clustering analysis and identified 2 groups, one with a high and one with a low proportion of EVT (Fig. 5B and Supplementary Table S2). The EVT^{lo} cases (n = 10) showed a high proportion and the EVT^{hi} cases (n = 6) showed a low proportion of STB signal in a similar comparison using the ratio of STB to all troph signal (Supplementary Table S2). The DEA of these 2 subpopulations showed that the EVT^{hi}/STB^{lo} cases were consistent with increased expression of EVT markers, *HLAG*, and *PLAC8*, whereas the EVT^{lo}/STB^{hi} cases showed increased expression of the STB marker *CSH1* (Supplementary Table S3), verifying that deconvolution reflects the cell type enrichments correctly. The gene ontology analysis revealed that the EVT^{hi}/STB^{lo} cases were significantly enriched with immune and inflammatory response pathways, whereas the EVT^{lo}/STB^{hi} cases were significantly enriched with growth hormone and nutrient signaling (Supplementary Fig. S2). We further evaluated the clinical characteristics of these 2 subgroups of PE placentas with MVM (Supplementary Table S12) and found that although all 16 cases in both the categories were associated with an SGA neonate, the EVT^{hi}/STB^{lo} cases showed a significantly lower birth weight percentile, suggesting these to be clinically more severe subtypes of PE with MVM, than the EVT^{lo}/STB^{hi} subtype. To validate the deconvolution data, we performed immunohistochemistry using an EVT marker (HLA-G) and an STB marker (CSH1) on all cases with available blocks (15 of the 16 cases) and noted distinct morphologies and staining patterns between the groups (Fig. 5C): the EVT^{hi}/STB^{lo} PE group showed patchy areas of HLA-G staining within the placental disc near foci of perivillous fibrin deposition, whereas the EVT^{lo}/STB^{hi} PE group showed HLA-G only in a few distinct intraplacental trophoblast islands within the villous tissue (Fig. 5C and Supplementary Fig. S3). Conversely, CSH1 staining revealed differences in the STB layer within these 2 groups of PE placentas, highlighting prominent syncytial knots in the EVT^{hi}/STB^{lo} cases, and a thick STB layer throughout the villous tissue in the EVT^{lo}/STB^{hi} PE cases (Fig. 5D and Supplementary Fig. S3).

In summary, these data indicate that PE placentas with MVM pathology show significant enrichment of inflammatory and hypoxia-associated pathways, with reduced cell proliferation, compared with nonhypertensive control placentas with MVM. In patients with PE and MVM who delivered preterm, there was an altered balance of terminally differentiated trophoblast, with distinct morphologies and staining patterns, which also represent different degrees of severity with respect to birth weight. These data point toward the heterogeneity of PE and the utility of morphologic, immunohistochemical, and transcriptomic assessments for dissecting such heterogeneity to identify the subgroups of the current clinically recognized categories of PE (Fig. 6).

Discussion

Thus far, there have been a limited number of studies that have integrated clinical history with placental pathology and transcriptomic profiling to identify the subgroups of PE. Our study aimed to approach this question comprehensively, integrating detailed clinical characterization with morphologic, immunohistochemical, and RNA profiling of placentas within a single-center cohort. Our analysis also applied the latest in-placental pathology subclassification system[19] and a state-of-the-art computational method (computational

deconvolution using cell type-specific signatures derived from single-cell RNA-seq data) for the analysis of bulk transcriptomic data.[44]

Our analysis of this complex disease began with subcategorization based on clinical features. Although patients with preexisting hypertension or proteinuria are at a higher risk of developing PE, it is still unclear as to what degree the pathophysiology of such "superimposed" PE overlaps with "primary" PE; hence, we decided to exclude patients with "superimposed" PE and focus on those with primary PE in the current study. As previously documented,[19,26–28] the pattern of placental injury most highly associated with PE was MVM, defined as a small placental disc with other features of underlying maternal vascular compromise, leading to accelerated maturation of the villous tree and infarcted tissue. However, MVM can of course coexist with other patterns of placental injury. In this study, we focused on the lesions of FVM and VUE because these have been described in association with PE.[62–65] Thus, we also evaluated cases of pure MVM, MVM + FVM, and MVM + VUE and noted that compared with the latter category, the cases of pure MVM and MVM + FVM are distinguished by earlier GA at delivery. In addition to earlier delivery, MVM, but not FVM, was associated with a high prevalence of SGA neonates; however, MVM + FVM, a pattern of injury more prevalent in our PE cohort, was also associated with SGA as a neonatal outcome. These findings are consistent with some[66] but differ from other studies[28,46,67] that have documented a clear association between FVM and the delivery of SGA neonates. The discrepancies among studies may have been due to slight differences in study design and definitions of FVM (ie, inclusion of low-grade and high-grade lesions).[19] It should be pointed out that although FVM in the current study included both low- and high-grade lesions, this category was composed of cases of pure FVM, excluding those with coexisting VUE or MVM. Recently, Freedman et al[28] performed a detailed analysis of all 4 patterns of placental injury (MVM, FVM, VUE, and ACA), including grading of these lesions, and evaluated the associations of various combinations of these patterns with preterm delivery and delivery of SGA neonates. Although the authors noted the highest risk of SGA to be associated with the presence of multiple high-grade lesions in the placenta (including MVM + FVM), they still found a slightly increased risk of SGA even with low-grade FVM (odds ratio, 1.9–3.7).[28] Regardless of these differences, however, both their study and ours point toward the utility of this pathologic framework in defining clinically significant patterns of placental injury, thus affirming the need to incorporate such placental pathologic data into pregnancy cohorts.

Following morphologic analysis, we used trophoblast lineage-specific markers to further evaluate the PE subtypes based on the patterns of placental injury. Specifically, there have been conflicting reports about the number of CTB, the proliferative progenitor cell type, in PE placentas, with some studies showing an increased CTB number[49,50] and others noting no differences compared with that of nonhypertensive control placentas.[48] Our results showed that overall, although there is no difference in the CTB number per villous area between the PE and nonhypertensive control samples when whole sections of placental disc are interrogated, regional differences in histopathologic patterns of placental injury can impact this finding; that is, the number of CTB per villous area may differ between affected and unaffected regions of the same placenta. Specifically, we found that placentas with FVM show loss of CTB in regions of AV, whereas those with VUE show an increase in CTB in

regions with CI. Although this finding needs to be further validated with larger numbers of such cases, our data strongly suggest that the histopathologic patterns of placental injury, over and above clinical disease, should be taken into account when evaluating cellular phenotypes in the placenta.

We next performed an RNA-seq analysis to explore the underlying molecular etiology of primary PE with MVM. Other studies have used RNA-seq for evaluating PE placentas; however, none has distinguished between primary and superimposed PE or selected cases and controls based on different pathologic patterns of placental injury.[68–70] Although this methodology resulted in a smaller number of samples evaluated (n = 18 for the nonhypertensive group and n = 26 for the PE group), this was still a larger sample size than 2 of the 3 previously published studies and, importantly, controlled for the histopathologic pattern of injury (MVM).[68,69] Interestingly, although both the cases and controls showed an MVM pattern of placental injury, the PE group (characterized by the presence of clinical signs and symptoms) still showed alterations in pathways associated with hypoxia and inflammation. This is consistent with a previous study that showed similarities in gene expression between PE placentas and placental explants exposed to low oxygen conditions.[71] Our results are also consistent with the proposed hypothesis that compared with small placentas from patients with normotensive fetal growth restriction, small placentas from patients with PE, particularly EO (preterm) PE, show evidence of oxidative stress, superimposed on endoplasmic reticulum stress, resulting in the release of proinflammatory cytokines and antiangiogenic factors.[72] That the nonhypertensive control group was enriched in pathways related to cell division and proliferation can be further connected to the low CTB number in the PE placentas from patients who delivered preterm and the enrichment of this cohort with the combined MVM + FVM pattern of placental injury.

Finally, recognizing the cellular heterogeneity contained in our placental samples, we used the single-cell placental transcriptomic data to further evaluate the phenotype of PE with MVM. Our data showed variability in the ratio of terminally differentiated trophoblast subtypes, with 2 distinct patterns (EVT^{lo}/STB^{hi} and EVT^{hi}/STB^{lo}) in the preterm PE group in contrast to a single pattern in the term PE group. We were able to validate these 2 different cellular phenotypes using immunostaining. Specifically, the EVT^{hi}/STB^{lo} cases showed patches of HLA-G^{+} cells near foci of perivillous fibrin deposition, a finding that has been noted in placentas in the setting of hypertensive disorders during pregnancy,[73] with a possible connection to the immunologic subtype of PE.[74] Of note, however, none of these cases met the criteria for massive perivillous fibrin deposition or maternal floor infarction (data not shown).[22] The cases with the converse (EVT^{lo}/STB^{hi}) pattern showed a thick STB layer throughout the chorionic villi, as noted using CSH1 staining. This is similar to previously reported thickening of the vasculosyncytial membrane in the setting of PE,[75] although it should be noted that the EVT^{hi}/STB^{lo} cases also showed abnormalities of the STB in the form of prominent syncytial knots, which may explain why these cases showed a more severe fetal growth restriction phenotype. Although abnormalities in the differentiation and maturation of the trophoblast have been associated with PE,[76,77] this is the first description of a disrupted balance of EVT and STB in the setting of a pregnancy-associated disorder. Considered together with the reduction in CTB number in preterm PE, it

could be hypothesized that a decreased or absent regenerative signal leads to premature loss of the trophoblast progenitor compartment, resulting in alterations in the balance of STB and EVT and, thus, placental dysfunction.

Although we made use of clinical, pathologic, cellular, and molecular data from our Perinatal Biorepository to understand PE, there were some limitations that deserve mention here. Our sample collection was selective, not only because of the fact that recruitment was limited to patients delivering at our university-affiliated hospitals, which are part of a regional tertiary care center and enriched for patients with high-risk pregnancies, but also because our study staff focused on consenting patients at a higher risk of adverse pregnancy outcomes. This likely resulted in some selection bias, as noted based on a cesarean section rate of ~50% in both our PE and nonhypertensive cohorts, which is significantly higher than the cesarean section rate of ~25% for our hospital system.[78] Another limitation of this study was that the diagnoses of hypertensive disease were made using retrospective chart reviews and, thus, may not be representative of actionable clinical information at the time of patient presentation/delivery. Our molecular (RNA-seq) analysis was also limited by the small sample number in each group; thus, future studies are needed with increased sample numbers, with the addition of RNA-seq analysis of groups with distinct pathologic patterns of placental injury, including pure versus mixed forms of MVM, FVM, and VUE.

The last decades have introduced large paradigm shifts, both in our clinical understanding of PE using the 2-stage theory of PE pathogenesis proposed in 1991[79] and, subsequently, based on the discovery, using molecular placental profiling, of a role of circulating antiangiogenic proteins in disease presentation.[80] We view the recent effort by the perinatal pathology community to standardize diagnoses of the patterns of placental injury as another potential paradigm shift in this field, filling the gap between clinical and molecular phenotyping of this complex disease in order to incorporate useful pathologic disease patterns into PE subclassification. We believe that this is an important step for not just comprehensive clinical phenotyping of this disease but also identification of cellular aberrations, which can hopefully be targeted for disease prevention or therapy in the near future.

Supplementary Material

Refer to Web version on PubMed Central for supplementary material.

Acknowledgments

The authors are very grateful to all patients who consented and donated placental tissues to the Perinatal Biorepository.

Funding

This work was supported by funds from the Eunice Kennedy Shriver National Institute of Child Health and Human Development (NICHD R01HD-089537 to M.M.P. and K99/R00 HD091452 to M.H.), California Institute for Regenerative Medicine Research and Training grant (TG2-01154 to M.H., the University of California San Diego), and the National Institutes of Health (NIH grant T32GM8806 to R.M.). The computational analysis was performed on Extreme Science and Engineering Discovery Environment Comet, which was supported by the National Science Foundation grant (ACI-1548562; allocation ID: TG-MCB140074).

Data Availability

RNA-seq data have been deposited to the Gene Expression Omnibus database under the accession number GSE186257.

References

1. American College of Obstetricians and Gynecologists. ACOG practice bulletin no. 202: gestational hypertension and preeclampsia. Obstet Gynecol. 2019;133(1):e1–e25. 10.1097/AOG.0000000000003018
2. Duley L The global impact of pre-eclampsia and eclampsia. Semin Perinatol. 2009;33(3):130–137. 10.1053/j.semperi.2009.02.010 [PubMed: 19464502]
3. Theilen LH, Meeks H, Fraser A, Esplin MS, Smith KR, Varner MW. Long-term mortality risk and life expectancy following recurrent hypertensive disease of pregnancy. Am J Obstet Gynecol. 2018;219(1):107.e1–107.e6. 10.1016/j.ajog.2018.04.002
4. Soto-Wright V, Bernstein M, Goldstein DP, Berkowitz RS. The changing clinical presentation of complete molar pregnancy. Obstet Gynecol. 1995;86(5):775–779. 10.1016/0029-7844(95)00268-V [PubMed: 7566847]
5. Steegers EA, Von Dadelszen P, Duvekot JJ, Pijnenborg R. Pre-eclampsia. Lancet. 2010;376(9741):631–644. 10.1016/S0140-6736(10)60279-6 [PubMed: 20598363]
6. August P, Sibai BM. Preeclampsia: clinical features and diagnosis. In: Lockwood CJ, ed. UpToDate. UpToDate, Inc; 2019.
7. Red-Horse K, Zhou Y, Genbacev O, et al. Trophoblast differentiation during embryo implantation and formation of the maternal-fetal interface. J Clin Invest. 2004;114(6):744–754. 10.1172/JCI22991 [PubMed: 15372095]
8. Huppertz B, Burton G, Cross JC, Kingdom JC. Placental morphology: from molecule to mother—a dedication to Peter Kaufmann—a review. Placenta. 2006;27(suppl A):S3–S8. 10.1016/j.placenta.2006.01.007 [PubMed: 16542720]
9. Ness RB, Roberts JM. Heterogeneous causes constituting the single syndrome of preeclampsia: a hypothesis and its implications. Am J Obstet Gynecol. 1996;175(5):1365–1370. 10.1016/s0002-9378(96)70056-x [PubMed: 8942516]
10. Lisonkova S, Joseph KS. Incidence of preeclampsia: risk factors and outcomes associated with early-versus late-onset disease. Am J Obstet Gynecol. 2013;209(6):544.e1–544.e12. 10.1016/j.ajog.2013.08.019
11. Dekker GA, Sibai BM. Etiology and pathogenesis of preeclampsia: current concepts. Am J Obstet Gynecol. 1998;179(5):1359–1375. 10.1016/s0002-9378(98)70160-7 [PubMed: 9822529]
12. Lachmeijer AM, Dekker GA, Pals G, Aarnoudse JG, ten Kate LP, Arngrímsson R. Searching for preeclampsia genes: the current position. Eur J Obstet Gynecol Reprod Biol. 2002;105(2):94–113. 10.1016/s0301-2115(02)00208-7 [PubMed: 12381470]
13. Skjaerven R, Vatten LJ, Wilcox AJ, Rønning T, Irgens LM, Lie RT. Recurrence of pre-eclampsia across generations: exploring fetal and maternal genetic components in a population based cohort. BMJ. 2005;331(7521):877. 10.1136/bmj.38555.462685.8F [PubMed: 16169871]
14. Masoudian P, Nasr A, de Nanassy J, Fung-Kee-Fung K, Bainbridge SA, El Demellawy D. Oocyte donation pregnancies and the risk of preeclampsia or gestational hypertension: a systematic review and metaanalysis. Am J Obstet Gynecol. 2016;214(3):328e339. 10.1016/j.ajog.2015.11.020 [PubMed: 26627731]
15. Giannakou K, Evangelou E, Papatheodorou SI. Genetic and non-genetic risk factors for pre-eclampsia: umbrella review of systematic reviews and meta-analyses of observational studies. Ultrasound Obstet Gynecol. 2018;51(6):720–730. 10.1002/uog.18959 [PubMed: 29143991]
16. Sovio U, Gaccioli F, Cook E, Hund M, Charnock-Jones DS, Smith GC. Prediction of preeclampsia using the soluble fms-like tyrosine kinase 1 to placental growth factor ratio: a prospective cohort study of unselected nulliparous women. Hypertension. 2017;69(4):731–738. 10.1161/HYPERTENSIONAHA.116.08620 [PubMed: 28167687]

17. Zeisler H, Llurba E, Chantraine F, et al. Predictive value of the sFlt-1:PlGF ratio in women with suspected preeclampsia. N Engl J Med. 2016;374(1):13–22. 10.1056/NEJMoa1414838 [PubMed: 26735990]
18. Andersen LL, Helt A, Sperling L, Overgaard M. Decision threshold for kryptor sFlt-1/PlGF ratio in women with suspected preeclampsia: retrospective study in a routine clinical setting. J Am Heart Assoc. 2021;10(17):e021376: 10.1161/JAHA.120.021376. [PubMed: 34459248]
19. Redline RW, Ravishankar S, Bagby CM, Saab ST, Zarei S. Four major patterns of placental injury: a stepwise guide for understanding and implementing the 2016 Amsterdam consensus. Mod Pathol. 2021;34(6):1074–1092. 10.1038/s41379-021-00747-4 [PubMed: 33558658]
20. Khong TY, Mooney EE, Ariel I, et al. Sampling and definitions of placental lesions: Amsterdam placental workshop group consensus statement. Arch Pathol Lab Med. 2016;140(7):698–713. 10.5858/arpa.2015-0225-CC [PubMed: 27223167]
21. Redline RW, Boyd T, Campbell V, et al. Maternal vascular underperfusion: nosology and reproducibility of placental reaction patterns. Pediatr Dev Pathol. 2004;7(3):237–249. 10.1007/s10024-003-8083-2 [PubMed: 15022063]
22. Kraus FT, Redline RW, Gersell DJ, Nelson DM, Dicke JM. Atlas of Nontumor Pathology: Placental Pathology. 1st ed. American Registry of Pathology and Armed Forces Institute of Pathology; 2004.
23. Redline RW, Ariel I, Baergen RN, et al. Fetal vascular obstructive lesions: nosology and reproducibility of placental reaction patterns. Pediatr Dev Pathol. 2004;7(5):443–452. 10.1007/s10024-004-2020-x [PubMed: 15547768]
24. Redline RW, Faye-Petersen O, Heller D, et al. Amniotic infection syndrome: nosology and reproducibility of placental reaction patterns. Pediatr Dev Pathol. 2003;6(5):435–448. 10.1007/s10024-003-7070-y [PubMed: 14708737]
25. Redline RW. Villitis of unknown etiology: noninfectious chronic villitis in the placenta. Hum Pathol. 2007;38(10):1439–1446. 10.1016/j.humpath.2007.05.025 [PubMed: 17889674]
26. Ernst LM. Maternal vascular malperfusion of the placental bed. APMIS. 2018;126(7):551–560. 10.1111/apm.12833 [PubMed: 30129127]
27. Helfrich BB, Chilukuri N, He H, et al. Maternal vascular malperfusion of the placental bed associated with hypertensive disorders in the Boston Birth Cohort. Placenta. 2017;52:106e113. Published correction appears in Placenta. 2019;86:52–53. 10.1016/j.placenta.2017.02.016 [PubMed: 28454692]
28. Freedman AA, Keenan-Devlin LS, Borders A, Miller GE, Ernst LM. Formulating a meaningful and comprehensive placental phenotypic classification. Pediatr Dev Pathol. 2021;24(4):337–350. 10.1177/10935266211008444 [PubMed: 33872108]
29. Roberts DJ, Post MD. The placenta in pre-eclampsia and intrauterine growth restriction. J Clin Pathol. 2008;61(12):1254–1260. 10.1136/jcp.2008.055236 [PubMed: 18641412]
30. Valensise H, Vasapollo B, Gagliardi G, Novelli GP. Early and late preeclampsia: two different maternal hemodynamic states in the latent phase of the disease. Hypertension. 2008;52(5):873–880. 10.1161/HYPERTENSIONAHA.108.117358 [PubMed: 18824660]
31. Leavey K, Bainbridge SA, Cox BJ. Large scale aggregate microarray analysis reveals three distinct molecular subclasses of human preeclampsia. PLoS One. 2015;10(2). 10.1371/journal.pone.0116508:e0116508. [PubMed: 25679511]
32. Leavey K, Benton SJ, Grynspan D, Kingdom JC, Bainbridge SA, Cox BJ. Unsupervised placental gene expression profiling identifies clinically relevant subclasses of human preeclampsia. Hypertension. 2016;68(1):137–147. 10.1161/HYPERTENSIONAHA.116.07293 [PubMed: 27160201]
33. Benton SJ, Leavey K, Grynspan D, Cox BJ, Bainbridge SA. The clinical heterogeneity of preeclampsia is related to both placental gene expression and placental histopathology. Am J Obstet Gynecol. 2018;219(6):604.e1–604.e25. 10.1016/j.ajog.2018.09.036
34. Gibbs I, Leavey K, Benton SJ, Grynspan D, Bainbridge SA, Cox BJ. Placental transcriptional and histologic subtypes of normotensive fetal growth restriction are comparable to preeclampsia. Am J Obstet Gynecol. 2019;220(1):110.e1–110.e21. 10.1016/j.ajog.2018.10.003

35. Hadlock FP, Harrist RB, Martinez-Poyer J. In utero analysis of fetal growth: a sonographic weight standard. Radiology. 1991;181(1):129–133. 10.1148/radiology.181.1.1887021 [PubMed: 1887021]
36. Blue NR, Savabi M, Beddow ME, et al. The Hadlock method is superior to newer methods for the prediction of the birth weight percentile. J Ultrasound Med. 2019;38(3):587–596. 10.1002/jum.14725 [PubMed: 30244476]
37. Pinar H, Sung CJ, Oyer CE, Singer DB. Reference values for singleton and twin placental weights. Pediatr Pathol Lab Med. 1996;16(6):901–907. 10.1080/15513819609168713 [PubMed: 9025888]
38. Dobin A, Davis CA, Schlesinger F, et al. STAR: ultrafast universal RNA-seq aligner. Bioinformatics. 2013;29(1):15–21. 10.1093/bioinformatics/bts635 [PubMed: 23104886]
39. Towns J, Cockerill T, Dahan M, et al. XSEDE: accelerating scientific discovery. Comput Sci Eng. 2014;16(5):62–74. 10.1109/MCSE.2014.80
40. Love MI, Huber W, Anders S. Moderated estimation of fold change and dispersion for RNA-seq data with DESeq2. Genome Biol. 2014;15(12):550. 10.1186/s13059-014-0550-8 [PubMed: 25516281]
41. Durinck S, Spellman PT, Birney E, Huber W. Mapping identifiers for the integration of genomic datasets with the R/Bioconductor package biomaRt. Nat Protoc. 2009;4(8):1184–1191. 10.1038/nprot.2009.97 [PubMed: 19617889]
42. Kuleshov MV, Jones MR, Rouillard AD, et al. Enrichr: a comprehensive gene set enrichment analysis web server 2016 update. Nucleic Acids Res. 2016;44(W1):W90–W97. 10.1093/nar/gkw377 [PubMed: 27141961]
43. Tsang JC, Vong JS, Ji L, et al. Integrative single-cell and cell-free plasma RNA transcriptomics elucidates placental cellular dynamics. Proc Natl Acad Sci U S A. 2017;114(37):E7786–E7795. 10.1073/pnas.1710470114 [PubMed: 28830992]
44. Newman AM, Liu CL, Green MR, et al. Robust enumeration of cell subsets from tissue expression profiles. Nat Methods. 2015;12(5):453–457. 10.1038/nmeth.3337 [PubMed: 25822800]
45. Wolf FA, Angerer P, Theis FJ. SCANPY: large-scale single-cell gene expression data analysis. Genome Biol. 2018;19(1):1–5. 10.1186/s13059-017-1382-0 [PubMed: 29301551]
46. Saleemuddin A, Tantbirojn P, Sirois K, et al. Obstetric and perinatal complications in placentas with fetal thrombotic vasculopathy. Pediatr Dev Pathol. 2010;13(6):459–464. 10.2350/10-01-0774-OA.1 [PubMed: 20438299]
47. Labarrere C, Althabe O. Chronic villitis of unknown aetiology and decidual maternal vasculopathies in sustained chronic hypertension. Eur J Obstet Gynecol Reprod Biol. 1986;21(1):27–32. 10.1016/0028-2243(86)90042-0 [PubMed: 3956826]
48. Jeschke U, Schiessl B, Mylonas I, et al. Expression of the proliferation markerKi-67 and of p53 tumor protein in trophoblastic tissue of preeclamptic, HELLP, and intrauterine growth-restricted pregnancies. Int J Gynecol Pathol. 2006;25(4):354–360. 10.1097/01.pgp.0000225838.29127.6 [PubMed: 16990712]
49. Arnholdt H, Meisel F, Fandrey K, Löhrs U. Proliferation of villous trophoblast of the human placenta in normal and abnormal pregnancies. Virchows Arch B Cell Pathol Incl Mol Pathol. 1991;60(6):365–372. 10.1007/BF02899568 [PubMed: 1683053]
50. Kaya B, Nayki U, Nayki C, et al. Proliferation of trophoblasts and Ki67 expression in preeclampsia. Arch Gynecol Obstet. 2015;291(5):1041–1046. 10.1007/s00404-014-3538-4 [PubMed: 25384521]
51. Lee Y, Kim KR, McKeon F, et al. A unifying concept of trophoblastic differentiation and malignancy defined by biomarker expression. Hum Pathol. 2007;38(7):1003–1013. 10.1016/j.humpath.2006.12.012 [PubMed: 17397906]
52. Liberzon A, Birger C, Thorvaldsdottir H, Ghandi M, Mesirov JP, Tamayo P. The molecular signatures database (MSigDB) hallmark gene set collection. Cell Syst. 2015;1(6):417–425. 10.1016/j.cels.2015.12.004 [PubMed: 26771021]
53. Rakner JJ, Silva GB, Mundal SB, et al. Decidual and placental NOD1 is associated with inflammation in normal and preeclamptic pregnancies. Placenta. 2021;105:23–31. 10.1016/j.placenta.2021.01.014 [PubMed: 33529885]

54. Flamant L, Roegiers E, Pierre M, et al. TMEM45A is essential for hypoxia-induced chemoresistance in breast and liver cancer cells. BMC Cancer. 2012;12(1):1–16. 10.1186/1471-2407-12-39 [PubMed: 22212211]
55. Rigourd V, Chauvet C, Chelbi ST, et al. STOX1 overexpression in choriocarcinoma cells mimics transcriptional alterations observed in preeclamptic placentas. PLoS One. 2008;3(12):e3905. 10.1371/journal.pone.0003905 [PubMed: 19079545]
56. van Dijk M, Oudejans CB. STOX1: key player in trophoblast dysfunction underlying early onset preeclampsia with growth retardation. J Pregnancy. 2011;2011:521826. 10.1155/2011/521826 [PubMed: 21490791]
57. Vaiman D, Calicchio R, Miralles F. Landscape of transcriptional deregulations in the preeclamptic placenta. PLoS One. 2013;8(6):e65498. 10.1371/journal.pone.0065498 [PubMed: 23785430]
58. Prieto-Fernández E, Egia-Mendikute L, Bosch A, et al. Hypoxia promotes syndecan-3 expression in the tumor microenvironment. Front Immunol. 2020;11:586977. 10.3389/fimmu.2020.586977 [PubMed: 33117401]
59. Gilkes DM, Bajpai S, Chaturvedi P, Wirtz D, Semenza GL. Hypoxia-inducible factor 1 (HIF-1) promotes extracellular matrix remodeling under hypoxic conditions by inducing P4HA1, P4HA2, and PLOD2 expression in fibroblasts. J Biol Chem. 2013;288(15):10819–10829. 10.1074/jbc.M112.442939 [PubMed: 23423382]
60. Xu R P4HA1 is a new regulator of the HIF-1 pathway in breast cancer. Cell Stress. 2019;3(1):27–28. 10.15698/cst2019.01.173 [PubMed: 31225497]
61. Xiong G, Stewart RL, Chen J, et al. Collagen prolyl 4-hydroxylase 1 is essential for HIF-1α stabilization and TNBC chemoresistance. Nat Commun. 2018;9(1):1–16. 10.1038/s41467-018-06893-9 [PubMed: 29317637]
62. Salafia CM, Pezzullo JC, Lopez-Zeno JA, Simmens S, Minior VK, Vintzileos AM. Placental pathologic features of preterm preeclampsia. Am J Obstet Gynecol. 1995;173(4):1097–1105. 10.1016/0002-9378(95)91333-5 [PubMed: 7485300]
63. Labarrere C, Althabe O. Chronic villitis of unknown etiology and maternal arterial lesions in preeclamptic pregnancies. Eur J Obstet Gynecol Reprod Biol. 1985;20(1):1–11. 10.1016/0028-2243(85)90077-2 [PubMed: 4029472]
64. Kim MJ, Romero R, Kim CJ, et al. Villitis of unknown etiology is associated with a distinct pattern of chemokine up-regulation in the feto-maternal and placental compartments: implications for conjoint maternal allograft rejection and maternal anti-fetal graft-versus-host disease. J Immunol. 2009;182(6):3919–3927. 10.4049/jimmunol.0803834 [PubMed: 19265171]
65. Benzon S, Zekić Tomaš S, Benzon Z, Vulić M, Kuzmic Prusac I. Involvement of T lymphocytes in the placentae with villitis of unknown etiology from pregnancies complicated with preeclampsia. J Matern Fetal Neonatal Med. 2016;29(7):1055–1060. 10.3109/14767058.2015.1032239 [PubMed: 25812675]
66. Hendrix ML, Bons JA, Alers NO, Severens-Rijvers CA, Spaanderman ME, Al-Nasiry S. Maternal vascular malformation in the placenta is an indicator for fetal growth restriction irrespective of neonatal birthweight. Placenta. 2019;87:8–15. 10.1016/j.placenta.2019.09.003 [PubMed: 31520871]
67. Gluck O, Schreiber L, Marciano A, Mizrachi Y, Bar J, Kovo M. Pregnancy outcome and placental pathology in small for gestational age neonates in relation to the severity of their growth restriction. J Matern Fetal Neonatal Med. 2019;32(9):1468–1473. 10.1080/14767058.2017.1408070 [PubMed: 29157050]
68. Sõber S, Reiman M, Kikas T, et al. Extensive shift in placental transcriptome profile in preeclampsia and placental origin of adverse pregnancy outcomes. Sci Rep. 2015;5(1):1–17. 10.1038/srep13336
69. Kaartokallio T, Cervera A, Kyllönen A, et al. Gene expression pro filing of preeclamptic placentae by RNA sequencing. Sci Rep. 2015;5:14107. Published correction appears in Sci Rep. 2016;6:17245. 10.1038/srep14107 [PubMed: 26388242]
70. Gong S, Gaccioli F, Dopierala J, et al. The RNA landscape of the human placenta in health and disease. Nat Commun. 2021;12(1):2639. 10.1038/s41467-021-22695-y [PubMed: 33976128]

71. Soleymanlou N, Jurisica I, Nevo O, et al. Molecular evidence of placental hypoxia in preeclampsia. J Clin Endocrinol Metab. 2005;90(7):4299–4308. 10.1210/jc.2005-0078 [PubMed: 15840747]
72. Burton GJ, Yung HW, Cindrova-Davies T, Charnock-Jones DS. Placental endoplasmic reticulum stress and oxidative stress in the pathophysiology of unexplained intrauterine growth restriction and early onset preeclampsia. Placenta. 2009;30:S43–S48. 10.1016/j.placenta.2008.11.003 [PubMed: 19081132]
73. Corrêa RR, Gilio DB, Cavellani CL, et al. Placental morphometrical and histopathology changes in the different clinical presentations of hypertensive syndromes in pregnancy. Arch Gynecol Obstet. 2008;277(3):201–206. 10.1007/s00404-007-0452-z [PubMed: 17786461]
74. Romero R, Whitten A, Korzeniewski SJ, et al. Maternal floor infarction/massive perivillous fibrin deposition: a manifestation of maternal antifetal rejection? Am J Reprod Immunol. 2013;70(4):285–298. 10.1111/aji.12143 [PubMed: 23905710]
75. Sankar KD, Bhanu PS, Kiran S, Ramakrishna BA, Shanthi V. Vasculosyncytial membrane in relation to syncytial knots complicates the placenta in preeclampsia: a histomorphometrical study. Anat Cell Biol. 2012;45(2):86–91. 10.5115/acb.2012.45.2.86 [PubMed: 22822462]
76. Redline RW, Patterson P. Pre-eclampsia is associated with an excess of proliferative immature intermediate trophoblast. Hum Pathol. 1995;26(6):594–600. 10.1016/0046-8177(95)90162-0 [PubMed: 7774887]
77. Leavey K, Benton SJ, Grynspan D, Bainbridge SA, Morgen EK, Cox BJ. Gene markers of normal villous maturation and their expression in placentas with maturational pathology. Placenta. 2017;58:52–59. 10.1016/j.placenta.2017.08.005 [PubMed: 28962696]
78. Pregnancy and childbirth. UC San Diego Health. Accessed October 12, 2021. https://health.ucsd.edu/specialties/obgyn/maternity/pages/quality.aspx
79. Redman CW. Current topic: pre-eclampsia and the placenta. Placenta. 1991;12(4):301–308. 10.1016/0143-4004(91)90339-h [PubMed: 1946241]
80. Maynard SE, Min JY, Merchan J, et al. Excess placental soluble fms-like tyrosine kinase 1 (sFlt1) may contribute to endothelial dysfunction, hypertension, and proteinuria in preeclampsia. J Clin Invest. 2003;111(5):649–658. 10.1172/JCI17189 [PubMed: 12618519]

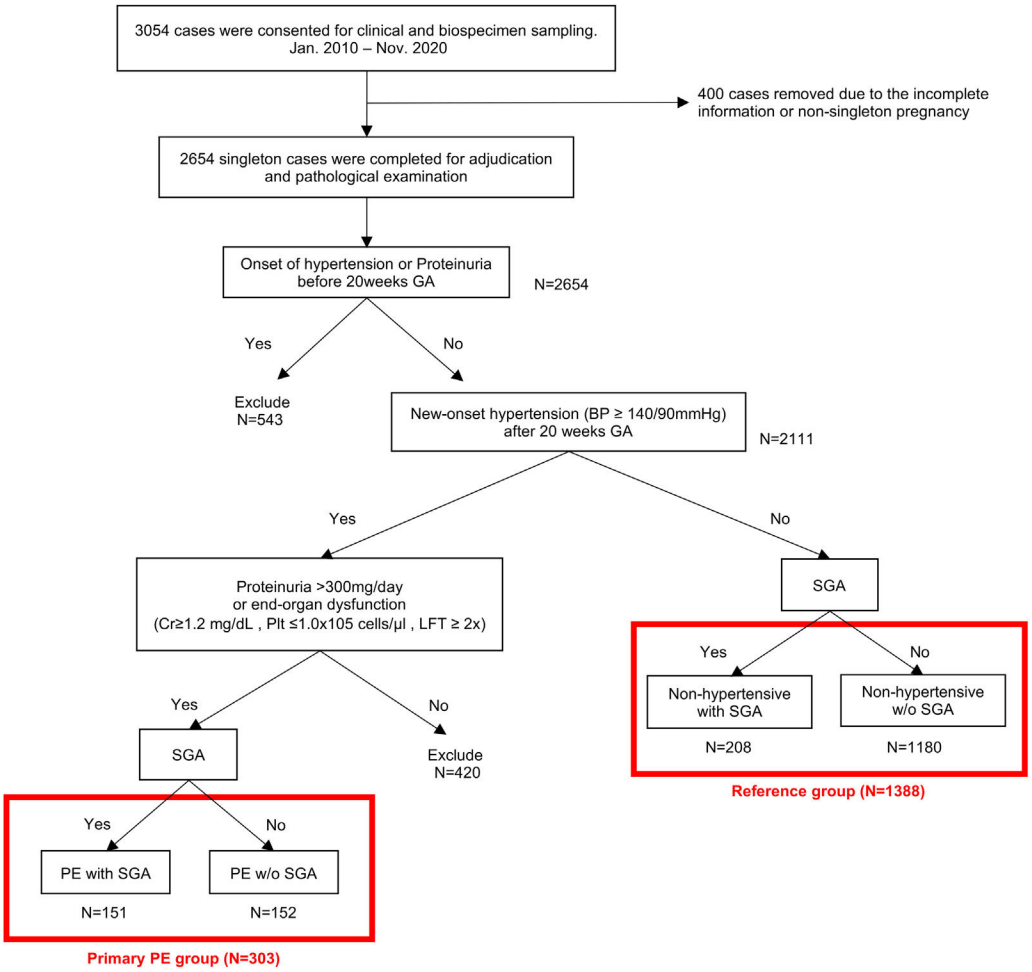

Figure 1.

Patient selection. Flow diagram demonstrating case selection from consent to data analysis. BP, blood pressure; Cr, creatinine; GA, gestational age; LFT, liver function test; LFT ≥ 2×, aminotransferase over twice the upper limit; PE, preeclampsia; Plt, platelet; SGA, small for gestational age; w/o, without.

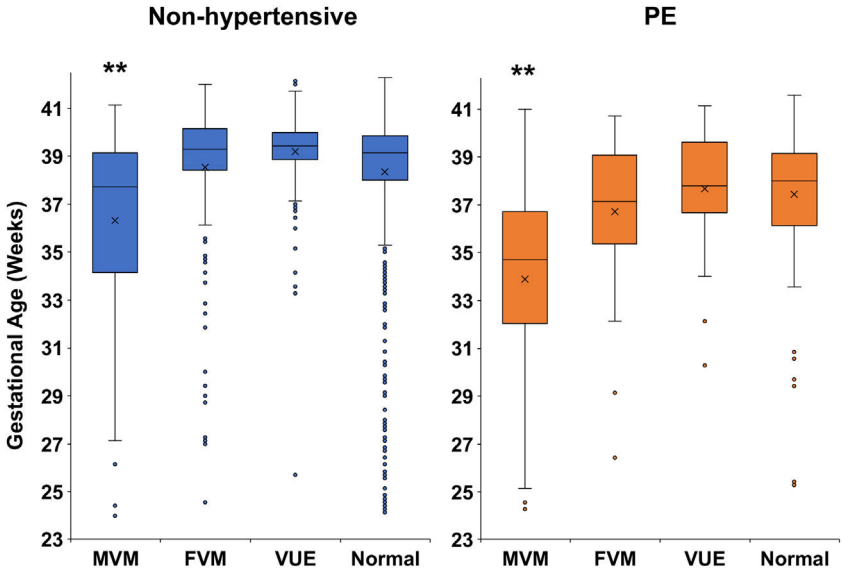

Figure 2.

Gestational age at delivery based on the presence of preeclampsia (PE) and specific pattern of placental injury. A box plot displaying gestational age (weeks) at delivery for the indicated pattern of placental injury. The Kruskal-Wallis pairwise test was used for statistical analysis, and Bonferroni correction was made to account for multiple comparisons. ** $P <$ .01. FVM, fetal vascular malperfusion; MVM, maternal vascular malperfusion; VUE, villitis of unknown etiology.

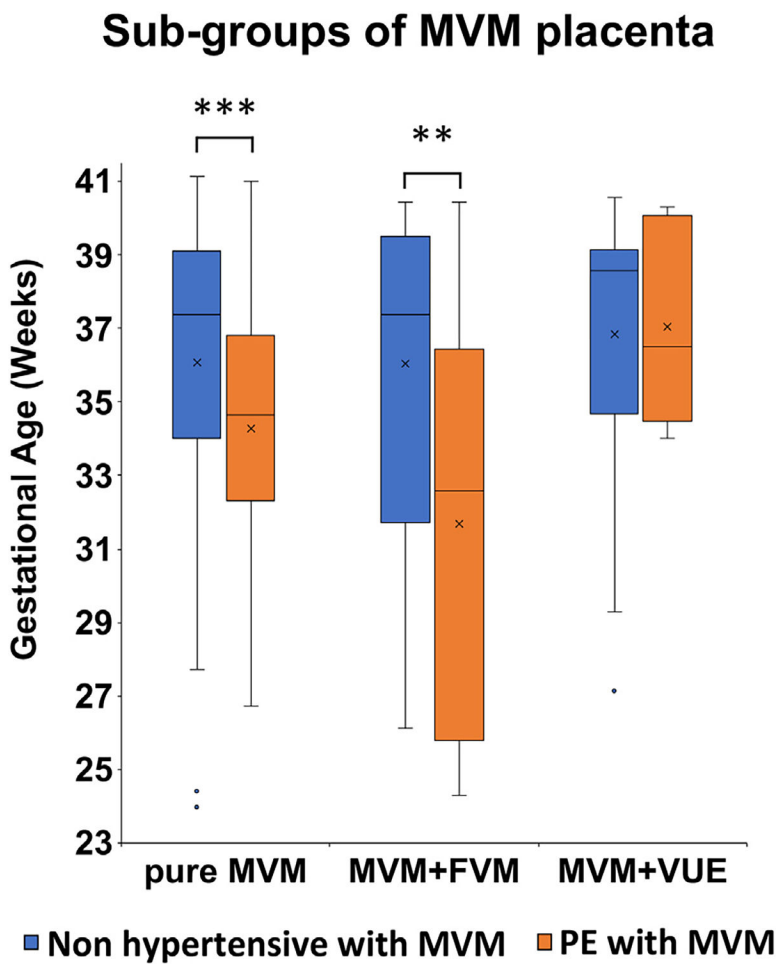

Figure 3.

Gestational age at delivery based on the presence of preeclampsia (PE) and subgroups of maternal vascular malperfusion (MVM) pattern of placental injury. A box plot displaying gestational age (weeks) at delivery and subgroups of MVM pattern of placental injury. Only cases that met the criteria for each subgroup of MVM were used in this analysis (Supplementary Tables S1 and S6). The Mann-Whitney *U* test was used for statistical analysis. $^{**}P < .01$, $^{***}P < .001$. FVM, fetal vascular malperfusion; PE, preeclampsia; VUE, villitis of unknown etiology.

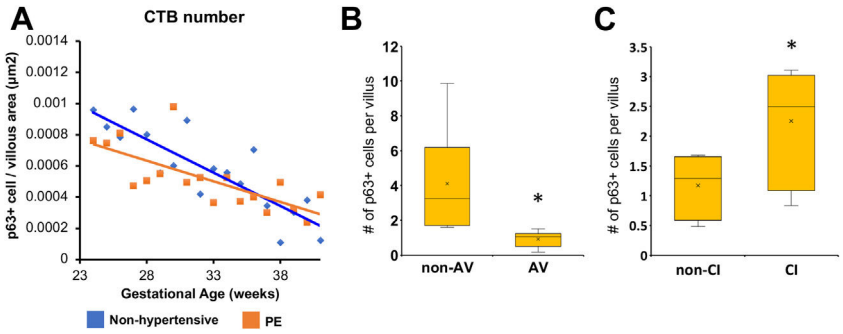

Figure 4.

Cytotrophoblast (CTB) number based on the presence of preeclampsia (PE) and specific patterns of placental injury. (A) A linear line is drawn based on the p63^{+} CTB number per villous area (µm^{2}) for each week of gestation (between 24 and 41 weeks) for the nonhypertensive control (blue, n = 99) and PE (orange, n = 91) groups. A linear regression model was used for the analysis. The plot displays only the median value at each gestational week. (B) A box plot displaying the number of p63^{+} CTB per villous area in 6 placentas from PE cases with avascular villi (AV) (as a hallmark of fetal vascular malperfusion [FVM]) (see the Case Selection section). Areas with and without AV were compared within each placenta; the paired *t* test was used to calculate the *P* value ($P = .04$). (C) A box plot displaying the number of p63^{+} CTB per villous area in 5 placentas from PE cases with villitis of unknown etiology (VUE). Areas with and without chronic inflammation (CI) were compared within each placenta; the paired *t* test was used to calculate the *P* values ($P = .01$).

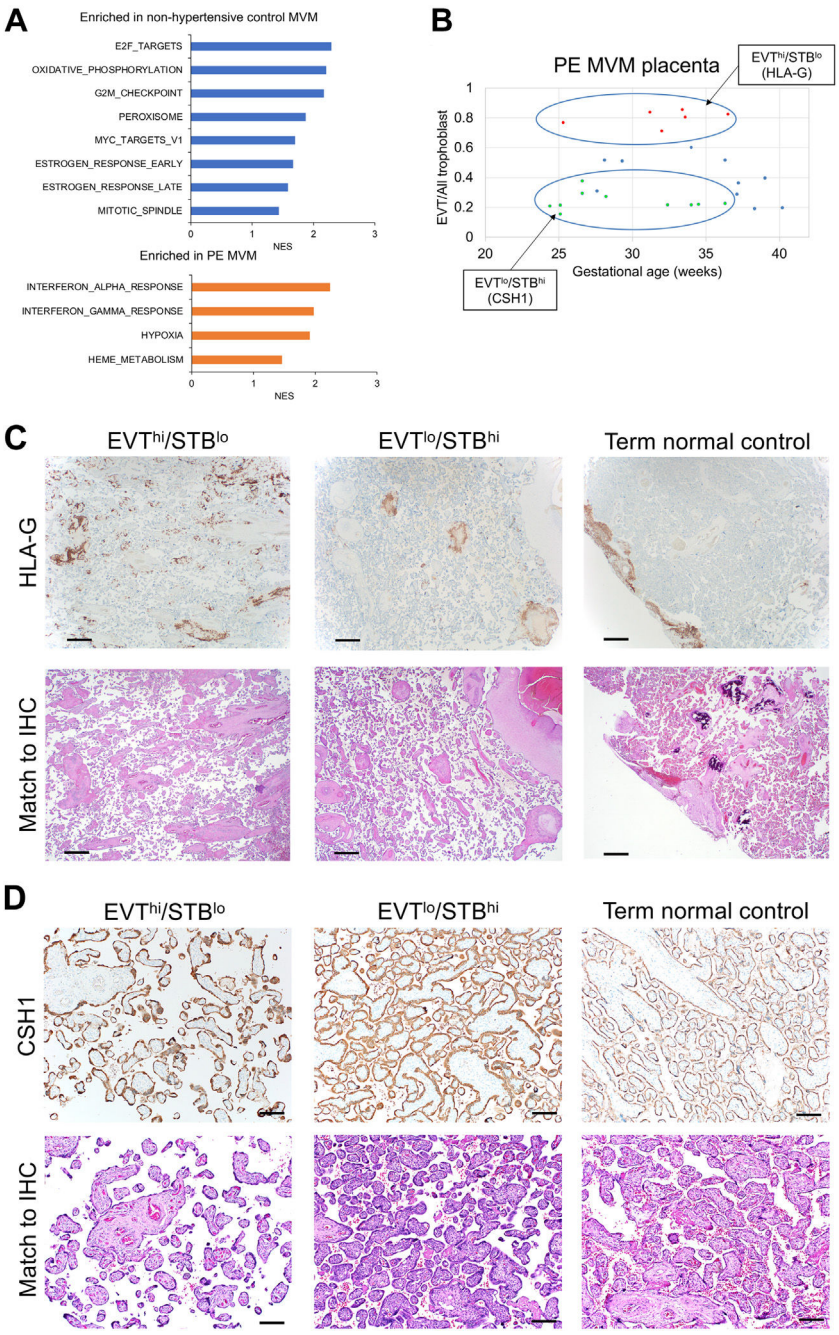

Figure 5.

The RNA sequencing-based analysis of preeclampsia (PE) and control placentas with maternal vascular malperfusion (MVM). (A) Gene set enrichment analysis of MVM placentas, comparing the PE and nonhypertensive control groups. Blue bars display the significant MSigDB hallmark gene sets enriched in the nonhypertensive control placentas with MVM, and orange bars show those enriched in PE placentas with MVM, with normalized enrichment score on the *x* axis. (B) CIBERSORT (cell-type identification by estimating relative subsets of RNA transcripts) output values of PE placentas with MVM were used to calculate the ratio of extravillous trophoblast (EVT) signal over

"all trophoblast" signal (the latter including sum of signals from the cytotrophoblast, syncytiotrophoblast [STB], and EVT) and plotted against gestational age. Two groups were identified within the preterm PE group: EVT^{hi}/STB^{lo} (red dots) and EVT^{lo}/STB^{hi} (green dots). Blue dots indicate the PE cases with MVM that did not fall into these 2 subgroups. A differential expression analysis was performed between these 2 groups, with major histocompatibility complex, class I, G (HLA-G) and chorionic omatomammotropin hormone 1 (CSH1) identified as key markers for each group. (C) Representative images from these 2 subgroups of preterm PE, along with the term nonhypertensive control group, stained with antibodies against the EVT marker, HLA-G (upper panels), with hematoxylin and eosin-stained image of the same region (lower panels). The bar represents 500 μm. (D) Representative images from these 2 subgroups of preterm PE, along with the term nonhypertensive control group, stained with antibodies against the STB marker, CSH1, or human placental lacorgen (upper panels), with hematoxylin and eosin-stained image of the same region (lower panels). The bar represents 500 μm. IHC, immunohistochemical.

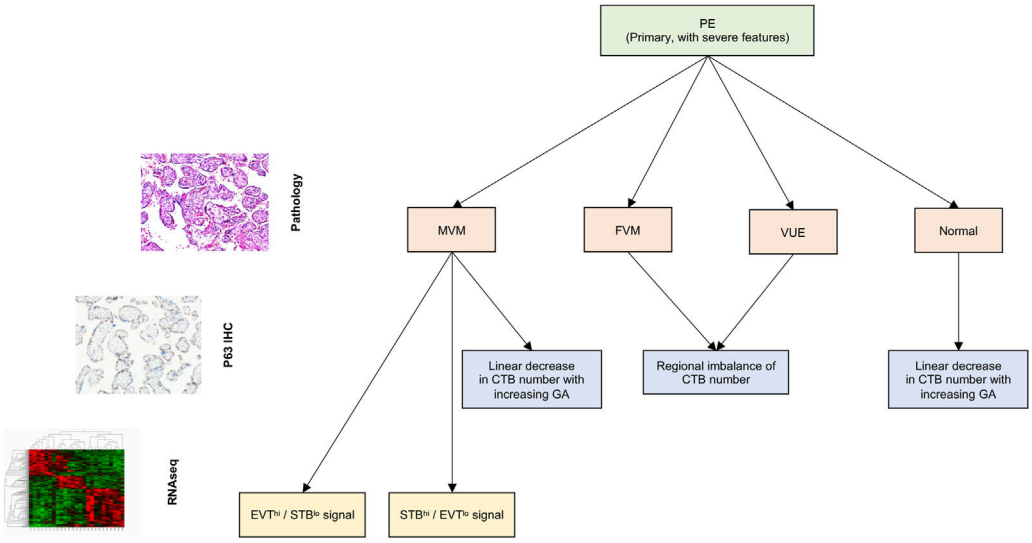

Figure 6.

Summary of progressive subtyping of primary preeclampsia with severe features based on sequential pathologic, immunohistochemical, and molecular analyses. CTB, cytotrophoblast; EVT, extravillous trophoblast; FVM, fetal vascular malperfusion; GA, gestational age; IHC, immunohistochemical; MVM, maternal vascular malperfusion; STB, syncytiotrophoblast; VUE, villitis of unknown etiology.

Table 1

Proportion of patterns of placental injury within the preeclampsia and control subgroups

Placental injury pattern	Nonhypertensive (n = 1388), n (%)	PE (n = 303), n (%)	*P*	Odds ratio (95% CI)
MVM	155 (11.2)	108 (35.6)	<.001***	4.406 (3.302–5.878)
FVM	163 (11.7)	29 (9.6)	.280	0.795 (0.525–1.017)
VUE	183 (13.2)	30 (9.9)	.119	0.724 (0.481–1.088)
Normal	887 (63.9)	136 (44.9)	<.001***	0.460 (0.358–0.592)

Pearson χ^2 test was used to calculate the *P* values.

FVM, fetal vascular malperfusion; MVM, maternal vascular malperfusion; PE, preeclampsia; VUE, villitis of unknown etiology.

*** $P < .001$.

Mod Pathol. Author manuscript; available in PMC 2023 April 07.

Table 2

Subgroups of maternal vascular malperfusion placenta

Placental injury pattern	Nonhypertensive with MVM (n = 155), n (%)	PE with MVM (n = 108), n (%)	*P*	Odds ratio (95% CI)
Pure MVM	104 (67.0)	68 (63.0)	.488	0.834 (0.498–1.395)
MVM + FVM	18 (11.6)	28 (25.9)	.003**	2.664 (1.386–5.119)
MVM + VUE	22 (14.2)	8 (7.4)	.089	0.484 (0.207–1.131)

Only cases that met the criteria for each subgroup of MVM were used in this analysis (Supplementary Table S1). The Pearson χ^2 test was used to calculate the *P* values.

FVM, fetal vascular malperfusion; MVM, maternal vascular malperfusion; PE, preeclampsia; VUE, villitis of unknown etiology.

** $P < .01$.